ELSEVIER

European Polymer Journal 36 (2000) 273–284

EUROPEAN POLYMER JOURNAL

Kinetic modelling of the thermal degradation of polyamide-6 nanocomposite

François Dabrowski, Serge Bourbigot*, René Delobel, Michel Le Bras

Laboratoire de Génie des Procédés d'Interactions Fluides-Matériaux (GéPRIM), E.N.S.C. Lille, USTL, BP 108, F-59652 Villeneuve d'Ascq Cedex, France

Received 27 January 1999; accepted 22 February 1999

Abstract

In this work, thermal behaviour of both polyamide-6 and polyamide-6 clay nanocomposite is studied. The Invariant Kinetic Parameters method enables modelling of the thermal degradation. The role played by oxygen during thermal degradation of polyamide-6 and polyamide-6 clay nanocomposite is investigated. The efficiency of the self-protective coatings which form during the pyrolysis and the thermo-oxidative degradation of polyamide-6 clay nanocomposite is discussed. The properties of these coatings are related to the previously observed improved fire properties of polyamide-6 clay nanocomposite as compared with polyamide-6. © 1999 Elsevier Science Ltd. All rights reserved.

1. Introduction

Polyamide resins are widely used as injected and extruding moulded materials especially for electrical applications, because of their particularly good mechanical properties.

The studies on nanocomposites began in the early 1980 s at Toyota Central Research Laboratories [1]. The first licensee of Toyota's nanocomposite technology was Ube Industries, which developed a polyamide clay nanocomposite. Recently other polymers have been tested as matrices: epoxy [2–4], polyether [5], poly(ethylene oxide) [6].

Le Bras et al. [7] have recently reported the effects of the addition of a natural clay filler in a polymeric system on its fire properties and demonstrated that LOI values are particularly improved by the addition of montmorillonite clay mineral. Montmorillonite is a particular type of smectite clay represented in Scheme 1 (from Gilman et al. [8,29]).

Polyamide-6 nanocomposite (clay mass fraction from 2 to 70 wt%) is synthesised by ring-opening polymerisation of ϵ-caprolactam in the presence of cation exchanged montmorillonite clay according to the reactions sequence presented in Scheme 2 (from Gilman et al. [8,29]). This process creates a polymer layered silicate nanocomposite with either an intercalated hybrid structure or a delaminated hybrid structure. The intercalated structure which forms when the clay mass fraction is greater than 20 wt% is characterised by a well ordered multilayer organisation with spacing between the silicate layers of only a few nanometers. The delaminated hybrid structure, which forms when the clay mass fraction is lower than 20 wt%, contains the silicate layers individually dispersed in the polymeric matrix. This nylon clay nanocomposite has already found two applications in the Far East: three-layer food packaging film for fresh meat and shock absorber for a laundry machine chamber.

* Corresponding author. Fax: +33-03-2043-6584.
E-mail address: serge.bourbigot@cnsc.lille.fr (S. Bourbigot).

0014-3057/99/$ - see front matter
PII: S0014-3057(99)00079-8

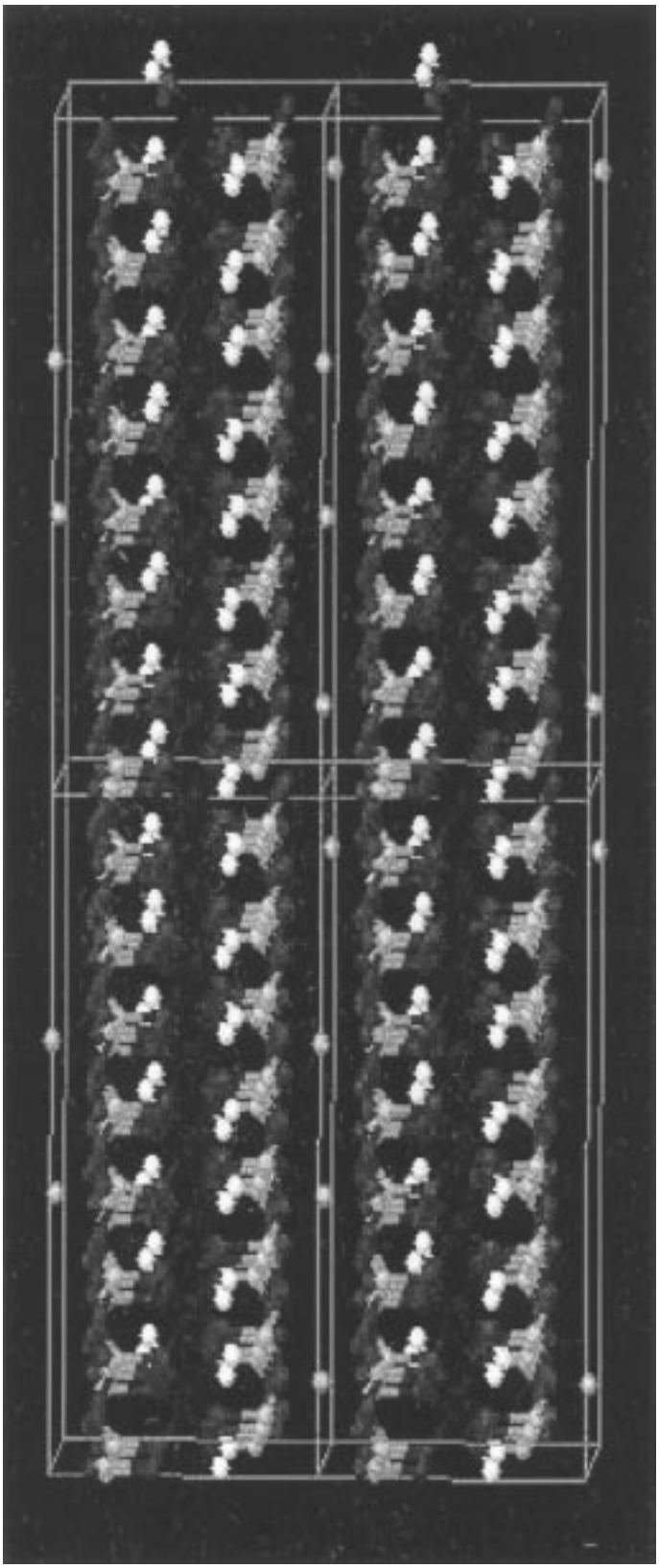

Scheme 1. Molecular representation of sodium montmorillonite, showing two alumino-silicate layers with the sodium cations in the interlayer gap or gallery (1.14 nm spacing between layers) (from Gilman et al. [8,29]).

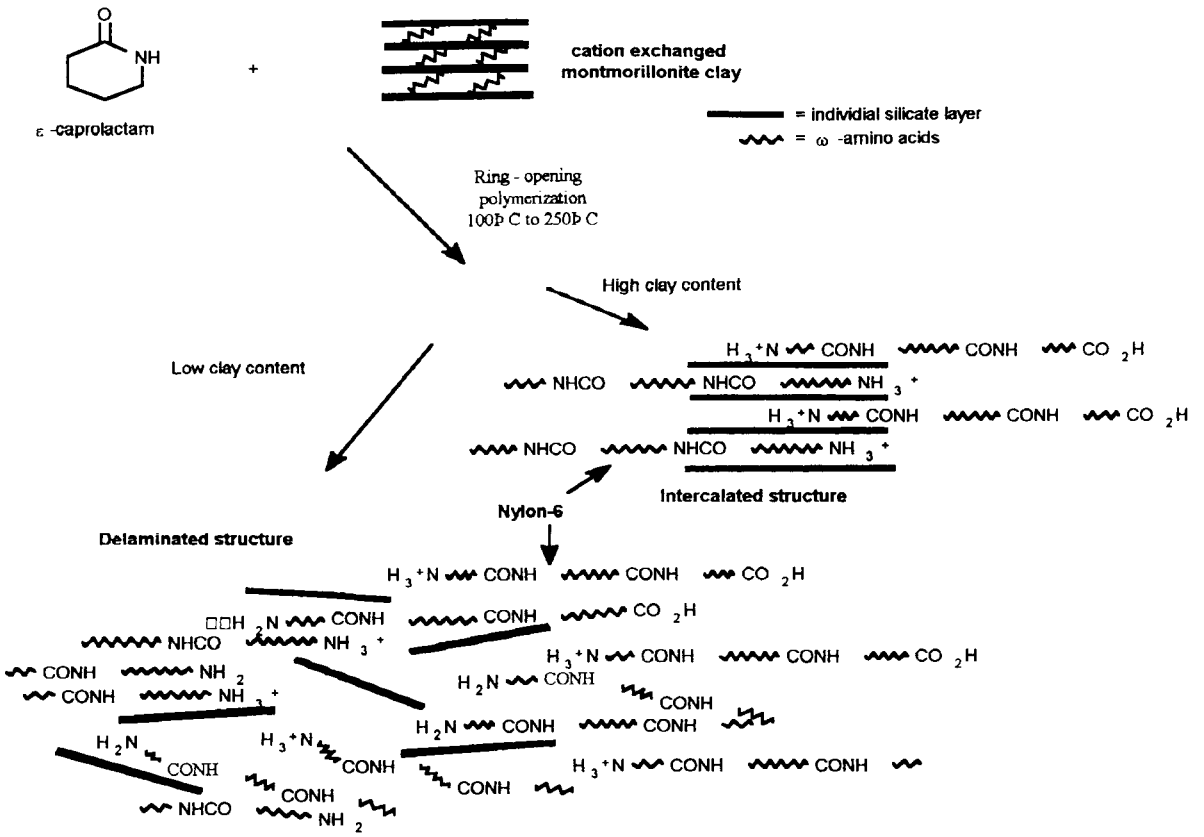

Scheme 2. Process used to prepare polymer layered silicate nanocomposites with either a delaminated structure or an intercalated structure (from Gilman et al. [8,29]).

The polymer layered silicate nanocomposite presents some improved physical properties [8–10,29]: the gas permeability of nylon clay nanocomposite is lower than that of nylon, nylon clay nanocomposite absorbs less moisture, the films of nylon clay nanocomposite are clear and nitro-cellulose ink printable. Moreover, Kojima et al. have reported improved mechanical properties [11]: polyamide-6 clay nanocomposite has improved strength modulus and distortion temperature compared with polyamide-6.

Gilman et al. have recently shown an improvement of the fire properties for a nylon nanocomposite with a relatively low clay weight fraction (5 wt%) as compared with a virgin PA-6: reduction in the peak of heat release rate by 63% without any increase of the soot and carbon monoxide levels evolved during combustion [8,29] (the degradation products of polyamide-6 have been discussed elsewhere [12]). Furthermore, contrary to fire retardants classically used, nanocomposites are environmentally friendly additives as they contain no halogen.

So, polyamide-6 clay nanocomposite worth additional working on its properties. The present work compares the pyrolysis and thermo-oxidative degradation of polyamide-6 and polyamide-6 clay nanocomposite.

The fire behaviour of a material depends on processes occurring in both condensed and gas phase and on the processes of heat and mass transfer. These processes strongly depend on the degradation reactions occurring in the condensed phase. Thus it is particularly interesting to model the thermal degradation of polyamide-6 clay nanocomposite. Nyden et al. previously chose to perform molecular dynamics simulation [13] of the thermal degradation of polypropylene/graphite rather than on nylon/clay nanocomposite because they "did not want to introduce any additional ambiguities into the interpretation of the computer simulations (quotation from reference [13])".

The strategy adopted in this work is to determine the kinetic parameters of the decomposition of polyamide-6 clay nanocomposite. But determining kinetic parameters from non-isothermal thermogravimetric analyses is a particularly difficult problem and it exists many calculation methods. In this work we have used a method

Table 1
The 18 different kinetic models used in this work

Kinetic models	$f_j(\alpha)$	$g_j(\alpha)$	
Nucleation and nucleus growing	$\frac{1}{n}(1-\alpha)\,(-\ln(1-\alpha))^{1-n}$	$(-\ln(-\alpha))^n$	S1—$n = 1/4$ S2—$n = 1/3$ S3—$n = 1/2$ S4—$n = 2/3$ S5—$n = 1$
Phase boundary reaction	$(1-\alpha)^n$	$1-(1-\alpha)$ $2[1-(1-\alpha)^{1/2}]$ $3[1-(1-\alpha)^{1/3}]$	S6—Plane symmetry S7—Cylindrical symmetry S8—Spherical symmetry
Diffusion	$\frac{1}{2}\alpha^{-1}$ $(-\ln(1-\alpha))^{-1}$ $\frac{3}{2}[(1-\alpha)^{-1/3}-1]^{-1}$ $\frac{3}{2}(1-\alpha)^{1/3}[(-\alpha)^{-1/3}-1]^{-1}$	α^2 $(1-\alpha)\ln(1-\alpha)+\alpha$ $1-\frac{2}{3}\alpha-(1-\alpha)^{2/3}$ $[(1-\alpha)^{1/3}-1]^2$	S9—Plane symmetry S10—Cylindrical symmetry S11—Spherical symmetry S18—Jander's type
Potential law	$\frac{1}{n}\alpha^{1-n}$	$\alpha^n (0 < n < 2)$	S12—$n = 1/4$ S13—$n = 1/3$ S14—$n = 1/2$ S17—$n = 3/2$
Reaction order	$\frac{1}{n}(1-\alpha)^{1-n}$	$1-(1-\alpha)^{1/2}$ $1-(1-\alpha)^{1/3}$	S15—$n = 1/2$ S16—$n = 1/3$

first proposed by Levchik et al. [14] and further developed in our laboratory by Bourbigot et al. [15] to determine the invariant kinetic parameters of the pyrolysis and of the thermo-oxidative degradation of polymers or fibres blends. These parameters are independent of the experimental conditions (especially of the heating rate) and no assumption is made concerning the kinetic degradation function. Therefore the results obtained are no longer apparent but are intrinsic characteristics of the system studied. Moreover the method enables to compute the distribution of probabilities associated to 18 kinetic functions ($f_j(\alpha)$) (Table 1) [15–16] and so to deduce the degradation mode of the material.

2. Experimental

2.1. Materials

Polyamide-6 and polyamide-6 clay nanocomposite (montmorillonite content: 2 wt%) were supplied by U.B.E. Industries as pellets. Powder (particles size lower than 200×10^{-6} m) for thermogravimetric (TG) analyses was obtained using a Retzsch cryogenic grinder at about -196°C.

2.2. Thermogravimetric analyses

TG analyses were performed using a Setaram MTB 10-8 thermobalance at five heating rates β_v (2.5; 5; 7.5; 10 and 15°C/min) from 20 to 800°C under air flow (Air Liquide grade, 5×10^{-7} m^3/s measured in standard conditions) and under nitrogen flow (N45 Air Liquide grade, 5×10^{-7} m^3/s measured in standard conditions). Samples (about 10^{-5} kg) were placed in vitreous silica pans. Precision on temperature measurements is $\pm$1,5°C.

2.3. IKP method

In this method we assume that the rate expression $d\alpha/dt$, where α is the degree of conversion, can be defined by:

$$d\alpha/dt = k \times f(\alpha)$$

with: $k = A \times \exp(-E/RT)$ according to the Arrhenius law.

Eighteen apparent activation energies (A_{jv}) and pre-exponential factors (E_{jv}) are calculated using the Coats and Redfern [17] method. The application of the IKP method is based on the study of the compensation effect [18,19]. For each function $f_j(\alpha)$, $\log(A_j)$ versus E_j is plotted and if a compensation effect is observed, a linear relation is observed [20] for each heating rate β_v and defined by the relation:

$$\log A_{jv} = B_v + l_v E_{jv}$$

where: A_{jv}, apparent pre-exponential factor calculated with a function $f_j(\alpha)$ at β_v, E_{jv}: calculated apparent activation energy.

A compensation effect of this kind is classified as false or as superficial [21] resulting from parameter distortion by an inappropriate kinetic model function [22].

The values of B_v and l_v are then calculated from the slopes and intercepts of the straight lines observed. The significance of B_v and l_v has been discussed by Lesnikovich et al. [20] and it has been demonstrated that:

$$B_v = \log\ (k_v)$$

$$l_v = (2{,}3RT_v)^{-1}$$

where k_v is the rate constant of the system at the temperature T_v, these two parameters being characteristics of the experimental conditions.

The curves log (k_v) are then plotted against $1/T_v$:

$$\log\ (k_v) = \log\ (A_{inv}) - E_{inv}/2.3RT_v$$

Thus, the values of the invariant activation energies and pre-exponential factors can be calculated from the slopes and intercepts of the curves.

The degradation is then modelled by computing the probabilities associated to eighteen degradation functions. The degradation of a polymeric material often cannot be represented by a single function but by a set of functions because of the different processes which can occur during the degradation of the material. Determination of invariant kinetic parameters and of probabilities for the degradation functions was carried out from the TG curves using software developed in our laboratory (software available from GéPRIM).

3. Results and discussion

The TG curves of polyamide and polyamide-6 clay nanocomposite for five heating rates under nitrogen are presented in Fig. 1 and under air in Fig. 2.

For polyamide-6 and polyamide-6 clay nanocomposite under both nitrogen and air, a first minor weight

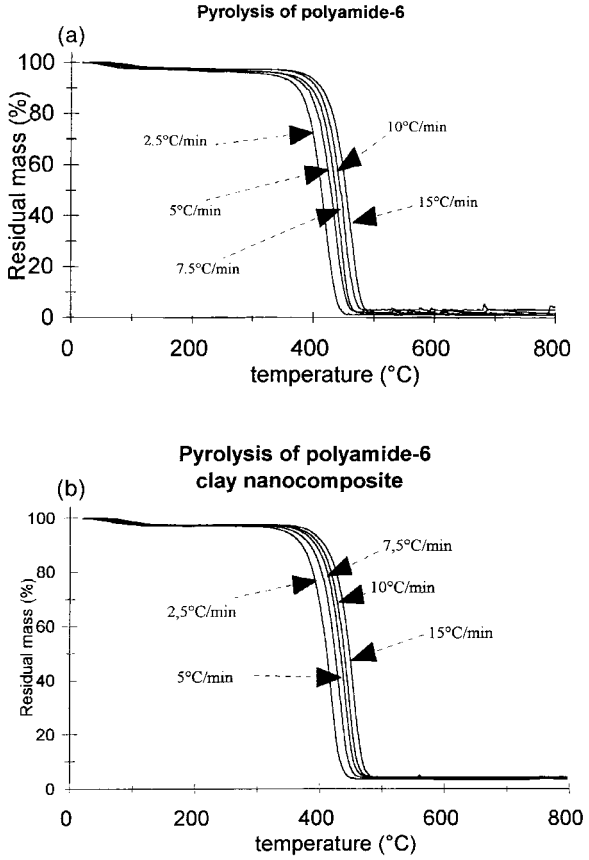

Fig. 1. TG curves of (a) polyamide-6 and (b) polyamide-6 clay nanocomposite under nitrogen.

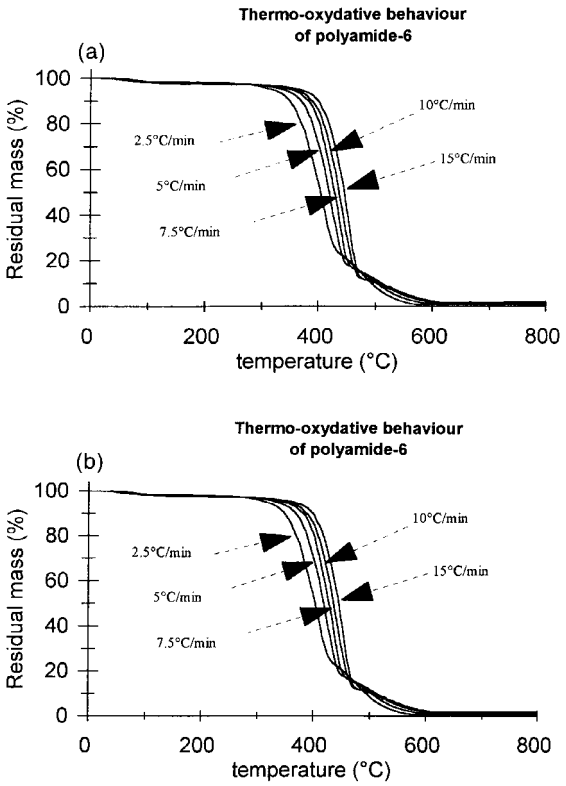

Fig. 2. TG curves under air of (a) polyamide-6 and (b) polyamide-6 clay nanocomposite.

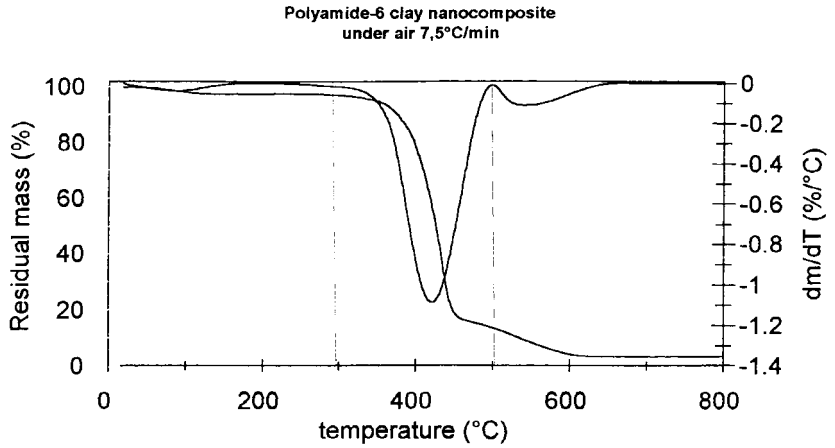

Fig. 3. Typical example of a TG and DTG curve: polyamide-6 clay nanocomposite under air; heating rate: 7.5°C/min.

loss is observed above 50°C. It can be assigned to the loss of physically sorbed water.

Under nitrogen the major stage of weight loss (about 93 wt% for polyamide-6 and about 91 wt% for polyamide-6 clay nanocomposite) occurs above 350°C and may be assigned to main-chain breakdown releasing water, NH_3, carbon monoxide and dioxide, and hydrocarbon fragments [12]. It leads to the formation of a charred residue (about 2 wt% for polyamide-6 and 4 wt% for polyamide-6 clay nanocomposite) stable up to 800°C.

Under air the major stage of weight loss (about 80 wt% for polyamide-6 and polyamide-6 clay nanocomposite) occurs between about 300 and 450°C. On further heating it leads to the formation of a stable carbonaceous material which then decomposes above 600°C leading to a stable charred residue (about 1 wt% for polyamide-6 and 3 wt% for polyamide-6 clay nanocomposite).

Whatever the atmosphere composition the mass difference between the high-temperature charred residue of polyamide-6 clay nanocomposite and of polyamide-6 corresponds to the weight content of the aluminosilicate structure in the polyamide-6 clay nanocomposite. Thus we may assume that the addition of nanocomposite structure does not stabilise the polymer above 500°C under nitrogen and above 600°C under air.

The IKP method is used to compute the invariant kinetic parameters and is applied to the temperature

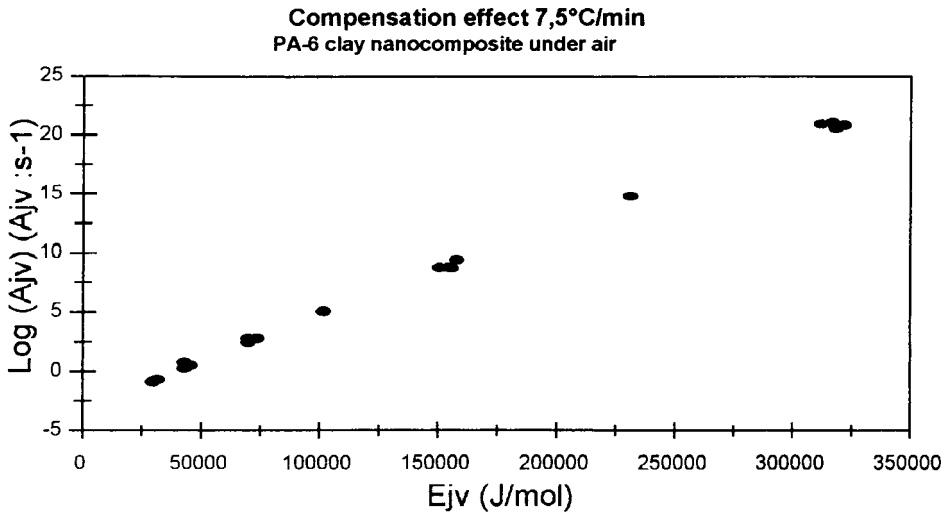

Fig. 4. Example of observed compensation effect between apparent activation energy and pre-exponential factor (PA-6 nanocomposite under air; heating rate 7.5°C/min).

Table 2
Invariant activation energies and pre-exponential factors of pyrolysis and thermo-oxydative degradation of polyamide-6 and polyamide-6 clay nanocomposite

	E_{inv} (kJ/mol)	$\log(A_{inv})$ (s^{-1})	Temperature range (K)
Polyamide-6 under nitrogen	180 ± 10	10.6	640–765
Polyamide-6 under air	250 ± 20	16.3	625–770
Polyamide-6 clay nanocomposite under nitrogen	200 ± 10	12.1	635–760
Polyamide-6 clay nanocomposite under air	300 ± 20	20.0	615–750

range shown in Fig. 3 corresponding to the major step of degradation of the material. Indeed, it is assumed that fuel formation and thus the resulting flammability of the material depend on this step.

The compensation effect is observed for each heating rate, material and gas flow (Fig. 4). The values of k_v at temperature T_v are then calculated from the slopes and intercepts of the straight lines.

Then the invariant kinetic parameters are computed (Table 2). Polyamide-6 and polyamide-6 clay nano-

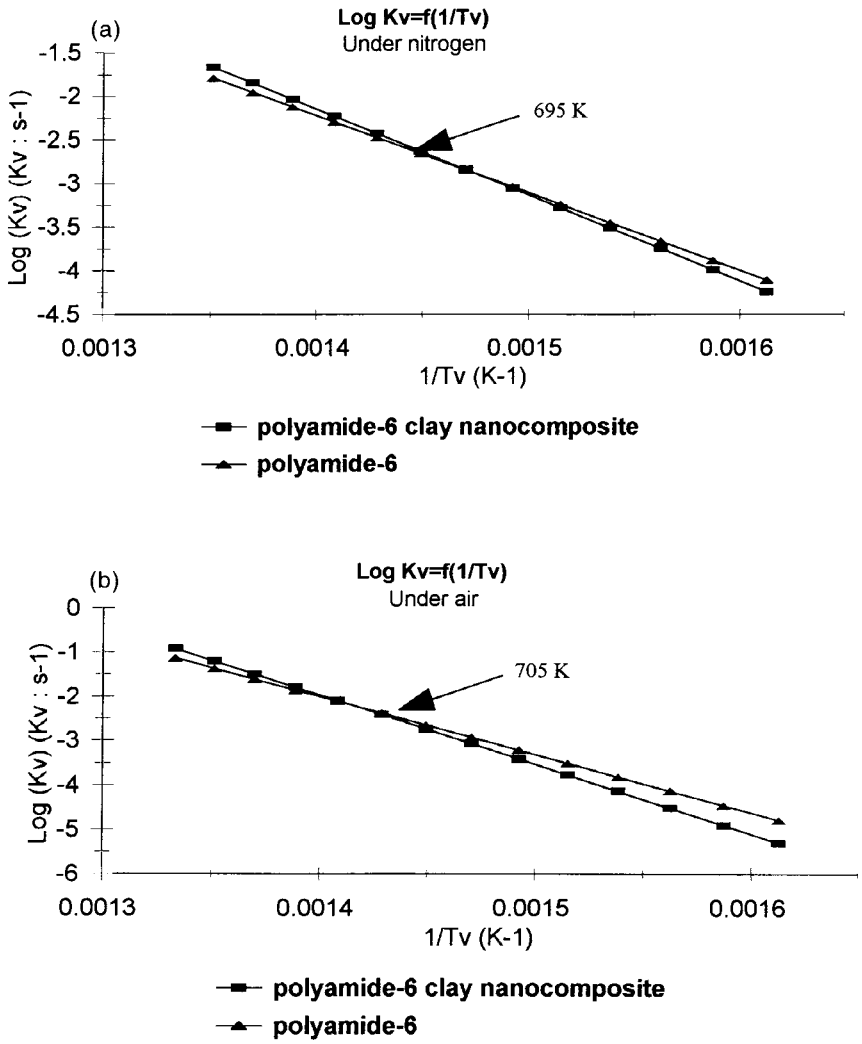

Fig. 5. Invariant rate constants versus temperature of polyamide-6 and polyamide-6 clay nanocomposite (a) under nitrogen and (b) under air.

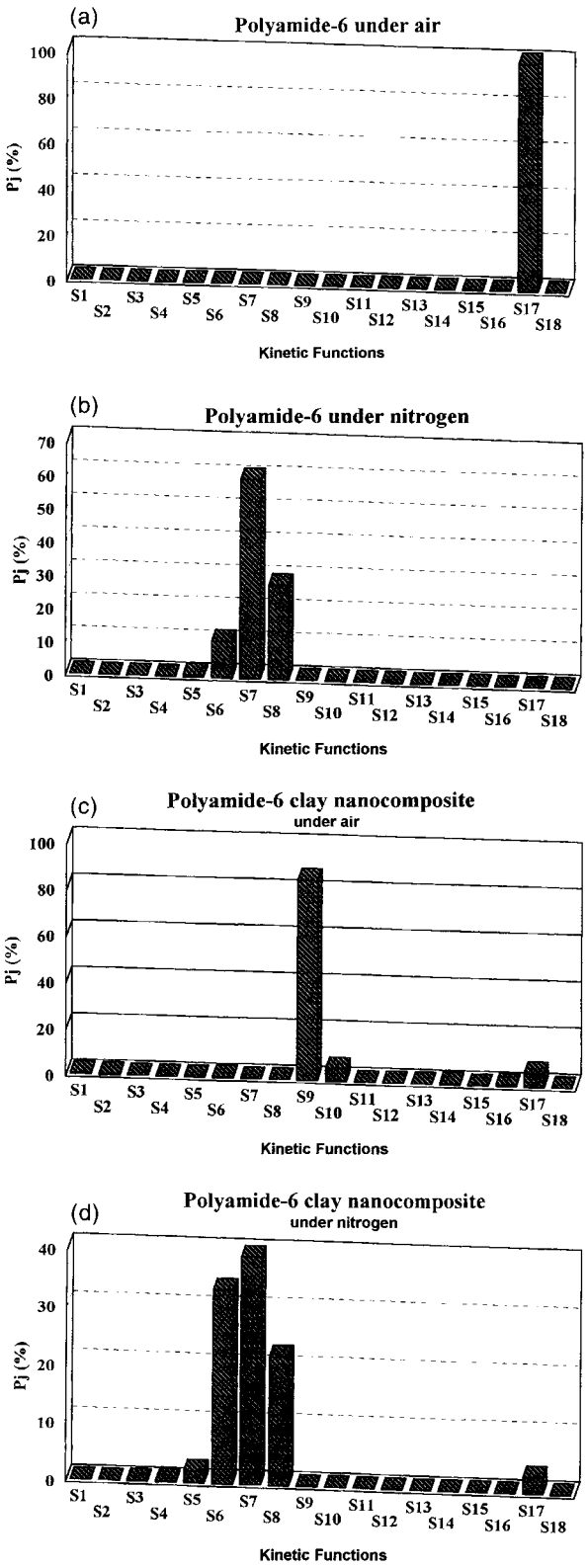

composite roughly have the same activation energy under nitrogen flow, whereas under air flow the activation energy of polyamide-6 clay nanocomposite is higher than that of polyamide-6. This result shows that oxygen plays a major role in the stabilisation process of polyamide-6 clay nanocomposite in comparison with polyamide-6.

The invariant rate constant K_v can be then plotted against temperature (Fig. 5):

$$\log\ (K_v) = \log\ (A_{inv}) - E_{inv}/(2.3RT_v)$$

The comparison of the invariant rate constants versus temperature allows a first comparison of the thermal stabilities of the materials. Under nitrogen and air, in the high temperature range, the decomposition rate of polyamide-6 clay nanocomposite is comparatively higher than the rate of polyamide-6. The intersection of the two straight lines is observed when T_v reaches about 695 K under nitrogen and 705 K under air.

The probabilities associated with the 18 degradation functions proposed from literature are presented in Fig. 6. The degradations of polyamide-6 and polyamide-6 clay nanocomposite under nitrogen are complex phenomena and must be represented by a set of functions. However under nitrogen, the degradations of polyamide-6 and polyamide-6 clay nanocomposite can mainly be represented by a combination of phase boundary reaction models in accordance with a degradation front model (hypothetical two-dimensional surface where the mass loss occurs) [23].

Under air flow the degradations of polyamide-6 and polyamide-6 clay nanocomposite are strongly modified. Thus oxygen plays a great role in the degradation process of both polyamide-6 and polyamide-6 clay nanocomposite. Under air the degradation of polyamide-6 can be represented by a potential law model corresponding to the classical degradation mode of a polymer. For polyamide-6 clay nanocomposite it can mainly be represented by a diffusion model with a plane symmetry, which would be in accordance with the formation of a physical barrier.

We may compare these results with the results previously obtained by Siat et al. on an industrial grade of polyamide-6 containing sized additives and/or fillers [24]. Under nitrogen flow the invariant activation energy of the degradation is higher in the present study and the thermal degradation can be more simply represented. Under air the invariant activation energies are nearly the same but in the present work the degradation can be represented by a potential law model

Fig. 6. Probability distribution of the kinetic degradation functions of polyamide-6 and polyamide-6 clay nanocomposite under air and nitrogen.

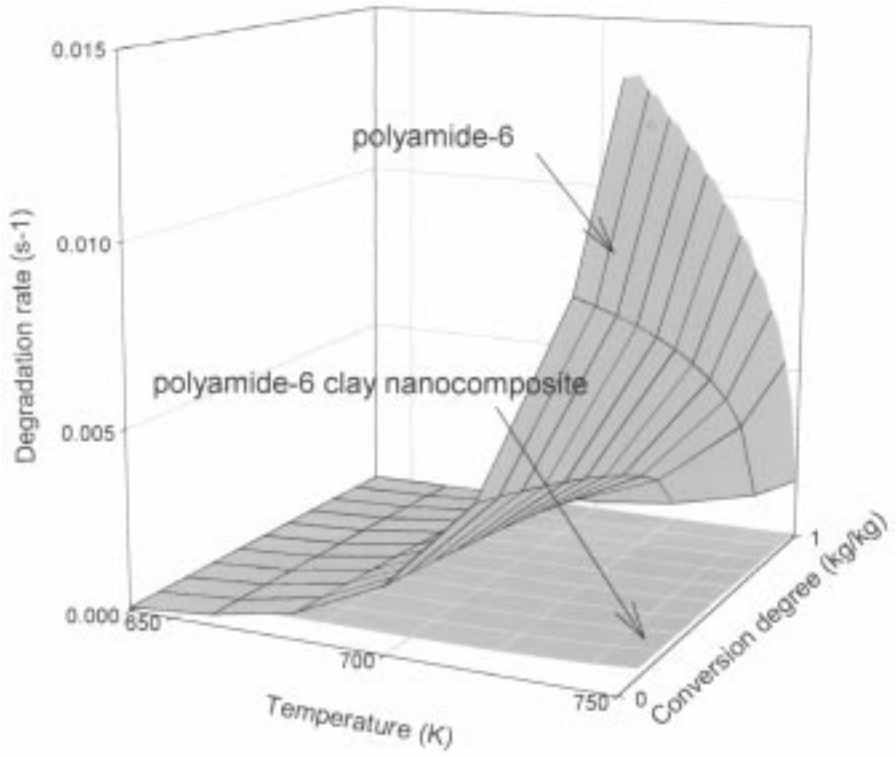

Fig. 7. Degradation rate of polyamide-6 and polyamide-6 clay nanocomposite under nitrogen versus temperature and conversion degree.

whereas it could be represented with a diffusion model in the Siat et al. study [24]. It may be proposed that the differences obtained between both materials are due to the presence of additives in the material used by Siat et al. [24] while polyamide-6 used in this study is 'pure'. This result implies that considering a polymer, the degradation process may be severely affected by the presence of fillers and so, cannot be deduced from previous studies on this polymer formulations.

The degradation rates V versus α and T where:

$$V = A_{\text{inv}} \times \exp(-E_{\text{inv}}/(RT)) \times \sum_{j=1 \text{ to } 18} f_j(\alpha)$$

are plotted against degradation rate and temperature in Figs. 7 and 8.

Under nitrogen whatever the temperature and conversion degree the degradation rate of polyamide-6 is higher than that of polyamide-6 clay nanocomposite. Under air flow polyamide-6 clay nanocomposite degrades more rapidly than polyamide-6 at high temperatures and then at lower temperatures and at high conversion degree polyamide-6 degrades more rapidly than polyamide-6 clay nanocomposite.

The probable degradation functions $f(\alpha)$ of both polyamide-6 and polyamide-6 clay nanocomposite under air and under nitrogen where:

$$f(\alpha) = \sum_{j=1 \text{ to } 18} P_j(\%) \times f_j(\alpha)$$

are presented in Fig. 9.

Under nitrogen the degradation functions of polyamide-6 and polyamide-6 clay nanocomposite versus conversion degree are roughly the same with a decrease in the degradation functions as the conversion degree increases: under isothermal conditions the rate of weight loss decreases as the conversion degree increases.

Under air the shapes of the degradation functions are modified. Polyamide-6 and polyamide-6 clay nanocomposite exhibit high values of their degradation functions (asymptotic behaviours) at low conversion degree which then decrease as the conversion degree rises. Therefore we can conclude that polyamide-6 clay

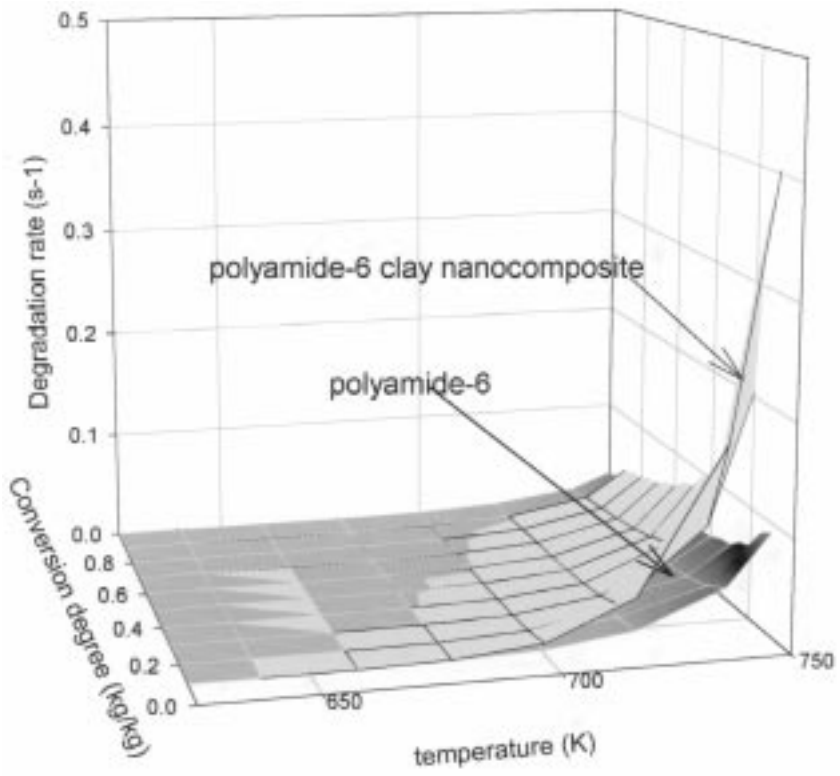

Fig. 8. Degradation rate of polyamide-6 and polyamide-6 clay nanocomposite under air versus temperature and conversion degree.

nanocomposite exhibits a self-protective behaviour leading to the formation of a protective barrier while the degradation function of polyamide-6 decreases at high conversion degrees (as an illustration, polyamide-6 clay nanocomposite exhibits a higher degradation function than polyamide-6 at low conversion degree ($\alpha < 0.55$) and then at high conversion degree ($\alpha > 0.55$) the degradation function of polyamide-6 is higher than that of polyamide-6 clay nanocomposite). The self-protective behaviour of polyamide-6 clay nanocomposite is observed (Fig. 8) for low conversion degree values when the temperature increases.

This kind of behaviour has already been discussed: ablative thermal degradation process in thermosets [23] and formation of a new material with fire retardant properties in intumescent thermoplastics [25].

Then heat and mass transfers may be modelled. For instance, kinetic data may be used in modelling of heat and mass transfer during combustion of an intumescent FR polymer, for instance using a model proposed by our laboratory [26–27] (this model based on the assumption that it exists an intumescent front analogous to the phase change process which can describe the fire behaviour of an intumescent material in the conditions of forced combustion).

4. Conclusion

The study shows that protective barriers are formed for polyamide-6 clay nanocomposite during its thermal degradation which slow down its rates of degradation via a diffusion process (lowers the escape of fuels). According to the shapes of the degradation functions and of the kinetic laws the coating formed by polyamide-6 clay nanocomposite may be assumed more efficient than that formed by polyamide-6. This could explain the improved fire properties of polyamide-6 clay nanocomposite compared with polyamide-6. The formation of a protective barrier in the case of polyamide-6 clay nanocomposite in fire conditions may also correspond to an already discussed change phase of the nanocomposite, from a delaminated structure to an intercalated structure [28]. This change phase enables an improved slow down of the escape of fuels [2,10]. Furthermore the results obtained demonstrate the essential role played by oxygen in the stabilisation process of nanocomposite in accordance with the results previously obtained by Gilman et al. using a cone calorimeter and a gasification apparatus [2].

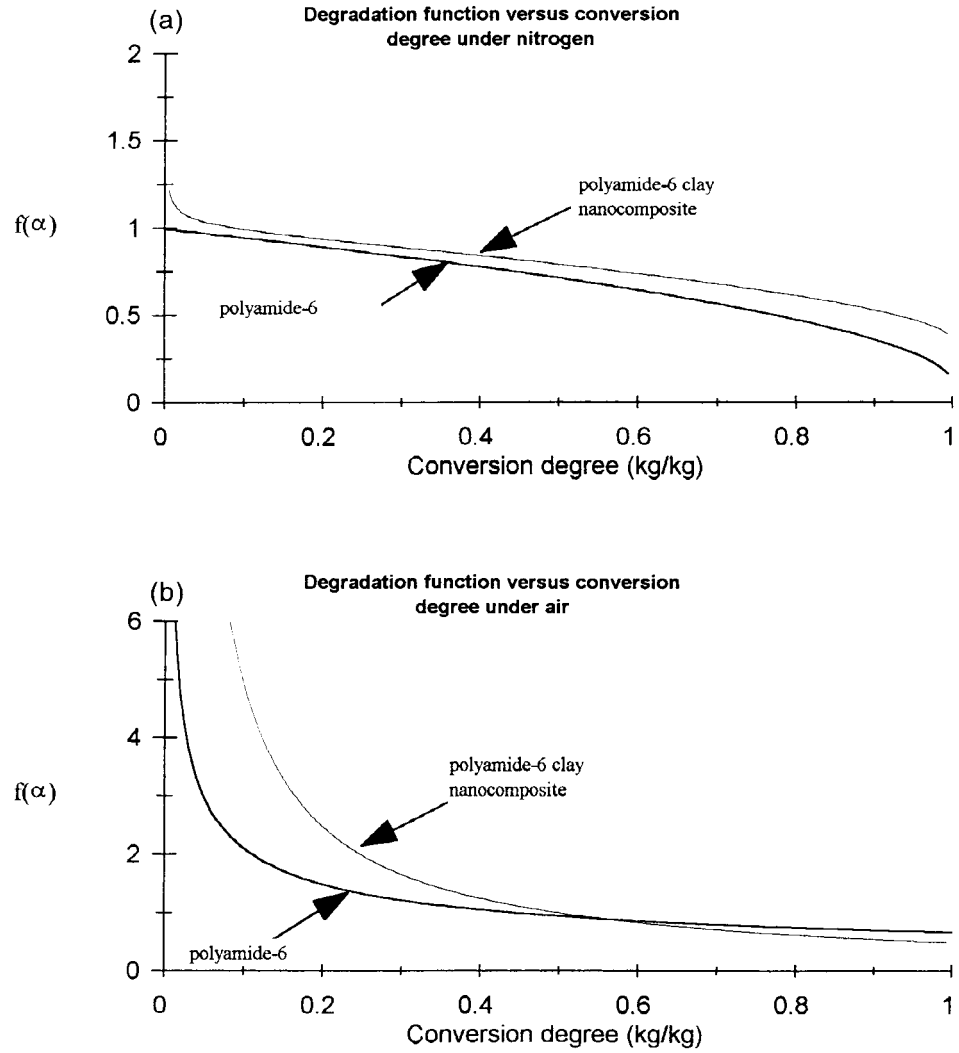

Fig. 9. Degradation function versus conversion degree of polyamide-6 and polyamide-6 clay nanocomposite (a) under nitrogen and (b) under air.

Acknowledgements

The authors gratefully acknowledge Dr Tabata (UBE Industries) for supplying raw materials. We are indebted to Dr J. W. Gilman (NIST, Gaithersburg MD) for helpful assistance and discussion.

References

[1] Gerard JF. Modern Plastics 1998;April:28–30.
[2] Lan T, Pinnavaia TJ. Chem Mater 1994;6:2216.
[3] Messersmith PB, Giannelis EP. Chem Mater 1994;6:1719.
[4] Wang MS, Pinnavaia TJ. Chem Mater 1994;6:468.
[5] Wu J, Lerner M. Chem Mater 1993;5:835.
[6] Aranda P, Ruiz-Hitzky E. Chem Mater 1992;4:1395.
[7] Le Bras M, Bourbigot S. Fire and Mat 1996;20:39.
[8] Gilman JW, Kashiwagi T, Giannelis EP, Manias E, Lomakin S, Lichtenhan JD, Jones P. In: Proceedings on the sixth European Meeting on Fire Retardancy of Polymeric Materials, Lille, France, September 1997.
[9] Giannelis EP. Adv Mater 1996;8:29.
[10] Kojima Y, Usuki A, Kawasumi M, Okada A, Kurauchi T, Kamigaito O. J Polym Sci: Part A: Polym Chem 1993;31:983.
[11] Kojima Y, Usuki A, Kawasumi M, Fukushima Y, Kurauchi T, Kamigaito O. J Mater Res 1993;8:1185.
[12] Hornsby PR, Wang J, Rothon R, Jackson G, Wilkinson G, Cossick K. Polym Deg Stab 1996;51:235.
[13] Nyden MR, Gilman JW. Comp Theor Polym Sci 1997;7(3/4):191.

[14] Levchik SV, Levchik GF, Lesnikovich AJ. Thermochim Acta 1985;77:157.
[15] Bourbigot S, Delobel R, Le Bras M, Normand D. J Chim Phys 1993;90:1909.
[16] Bourbigot S, Delobel R, Le Bras M, Schmidt Y. J Chim Phys 1992;89:1835.
[17] Coats AW, Redfern JP. Nature 1964;201:68.
[18] Nikoalev AV, Logvimenko VA, Gorberchev VM. J Therm Anal 1974;6:473.
[19] Criado JM, Gonzales M. Thermochim Acta 1981;46:201.
[20] Lesnikovich AI, Levchik SV, Guslev VG. Thermochim Acta 1984;77:357.
[21] Koga N, Sestak J. J Therm Anal 1991;37:1103.
[22] Koga N, Sestak J, Malek J. Thermochim Acta 1991;182:333.
[23] Le Bras M, Rose N, Bourbigot S, Henry Y, Delobel R. J Fire Sci 1996;14:199.
[24] Siat C, Bourbigot S, Le Bras M. Polym Deg Stab 1997;58:303.
[25] Bourbigot S, Delobel R, Le Bras M, Normand D. J Chim Phys 1993;90:1909.
[26] Bourbigot S, Duquesne S, Leroy JM. J Fire Sci, in press.
[27] Duquesne S, Bourbigot S, Leroy JM. Fire Chemistry Discussion Group, Nottingham, UK, November 1998.
[28] Gilman JW, Kashiwagi T, Lichtenhan JD. SAMPE J 1997;33:40.
[29] Gilman JW, Kashiwagi T, Giannelis EP, Manias E, Lomakin S, Lichtenhan JD, Jones P. In: Le Bras M, Camino G, Bourbigot S, Delobel R, editors. Fire Retardancy of Polymers The Use of Intumescence, vol. 203. Cambridge (UK): Royal Chem. Soc, 1998.